

Approximate Time-Optimal Trajectories for Damped Double Integrator in 2D Obstacle Environments under Bounded Inputs

Vishnu S. Chipade and Dimitra Panagou

Abstract—This article provides extensions to existing path-velocity decomposition based time optimal trajectory planning algorithm [1] to scenarios in which agents move in 2D obstacle environment under double integrator dynamics with drag term (damped double integrator). Particularly, we extend the idea of tangent graph [2] to \mathcal{C}^1 -Tangent graph to find continuously differentiable (\mathcal{C}^1) shortest path between any two points. \mathcal{C}^1 -Tangent graph has continuously differentiable (\mathcal{C}^1) path between any two nodes. We also provide analytical expressions for a near time optimal velocity profile for an agent moving on these shortest paths under damped double integrator with bounded acceleration.

Index Terms—time-optimal control, trajectory planning, double integrator with drag.

I. INTRODUCTION

Trajectory planning is a very important problem for autonomous robots. A significant body of literature is available that solves the problem of trajectory planning [3]. For obstacle environments, authors in [1] have proposed a method called path-velocity decomposition for trajectory planning. In this article, we consider the idea of path-velocity decomposition [1] to find time-optimal trajectory for an agent operating under double integrator dynamics with drag term (damped double integrator) to move from one point to another in an obstacle environment. The path-velocity decomposition approach [1] as the name suggests decomposes the trajectory planning problem in two sub-problems: 1) finding a path that avoids collision with static obstacles (path planning), 2) finding velocity profile on the path obtained in 1) to avoid moving obstacles (velocity planning). In [1], V-Graph (vertex graph) is used to find shortest path between to points in polygonal obstacle environment while a simple single integrator model with bounded speed is used to determine the a feasible time optimal velocity profile on the shortest path.

A better graph representation of an obstacle environment called Tangent graph, which is graph of consisting of common tangents of the polygonal obstacles in an environment is used in [2] for path planning. However, the paths obtained using Tangent graph are only continuous and not necessarily continuously differentiable (\mathcal{C}^1). We build upon

The authors are with the Department of Aerospace Engineering, University of Michigan, Ann Arbor, MI, USA; (vishnuc, dpanagou)@umich.edu

This work has been funded by the Center for Unmanned Aircraft Systems (C-UAS), a National Science Foundation Industry/University Cooperative Research Center (I/UCRC) under NSF Award No. 1738714 along with significant contributions from C-UAS industry members.

the idea of tangent graph to find \mathcal{C}^1 -Tangent graph by considering \mathcal{C}^1 boundaries around the polygonal obstacles in the environment. The \mathcal{C}^1 -Tangent graph consists of common tangents to the continuous closed convex boundaries around the polygonal obstacles and there exists a \mathcal{C}^1 path between any two nodes on the \mathcal{C}^1 -Tangent graph. This allows us to plan paths for agents moving under second order dynamics. We provide a novel quadratic function to systematically find the common tangents of the \mathcal{C}^1 boundaries of the obstacle.

Authors in [4] propose two filters: ellipse and convex-hull filter to reduce the search space for finding the shortest paths in the presence of circular obstacles. In this article, we extend the ellipse filter to more generic polygonal obstacles to reduce the search space so that more general obstacle environments can be considered.

In [5], the authors compute a time-optimal velocity profile for following a given path by meticulously keeping track of the lowest bound on the maximum speed and acceleration along the path, while maintaining the overall constant bound on the components of the acceleration vector and velocity vector. However, this approach requires several forward and backward numerical integration of the system dynamics, therefore can be computationally time intensive and also it would result in sub-optimal velocity profiles when euclidean norm constraints are to be considered on the acceleration. Compared to [5], in this article, we consider euclidean norm constraints on the acceleration input which is typical for many under actuated systems and we design near time-optimal velocity¹ profiles for agents moving under damped double integrator for which analytical expressions can be provided saving on computational time.

In summary, the contributions of this article are as follows:

- 1) derivation of continuous (\mathcal{C}^0), near time-optimal velocity profiles for agents moving under damped double integrator dynamics, so that they travel along the shortest paths between the given initial and final points while satisfying acceleration bounds;
- 2) derivation of a novel quadratic function to find the common tangents of two continuously differentiable (\mathcal{C}^1), closed, convex curves that approximate the polygonal obstacles;

¹Near time-optimal in this paper means actual travel time τ satisfies $\tau^* \leq \tau \leq (1 + \varepsilon)\tau^*$ where τ^* is the optimal travel time and $\varepsilon \ll 1$ is a small, positive constant.

- 3) an extension of ellipse filter [4] for general convex polygonal obstacles to reduce the search space to find the shortest paths between any two nodes on \mathcal{C}^1 -Tangent Graph.

A. Organization

The rest of the article is structured as follows: Section II provides the mathematical modeling and problem statement. In Section III, we give an overview of the path-velocity decomposition method to find near time-optimal trajectory in obstacle environment. Section IV provides details on \mathcal{C}^1 -Tangent graph and shortest paths. In Section III we provide analytical expression to find near time optimal velocity profile on given shortest path and the article in concluded in Section VI.

II. MODELING AND PROBLEM STATEMENT

We consider an agent moving under double integrator dynamics with a quadratic drag term (damped double integrator):

$$\begin{aligned} \dot{\mathbf{r}} &= \mathbf{v}, \\ \dot{\mathbf{v}} &= \mathbf{u} - C_D \|\mathbf{v}\| \mathbf{v}; \end{aligned} \quad (1)$$

$C_D > 0$ is the known, constant drag coefficient, $\mathbf{r} = [x \ y]^T$ is the position vector $\mathbf{v} = [v_x \ v_y]^T$, is the velocity vector, and $\mathbf{u} = [u_x \ u_y]^T$ is the acceleration of the agent, which serve also as the control input, all resolved in a global inertial frame $\mathcal{F}_{gi}(\hat{\mathbf{i}}, \hat{\mathbf{j}})$ (see Fig.2). The acceleration \mathbf{u} is bounded as:

$$\|\mathbf{u}\| \leq \bar{u}. \quad (2)$$

The dynamics in (1) take into account the air drag experienced by the agents modeled as a quadratic function of the velocity. Note also that the above damped double integrator inherently poses a speed bound on the agent under a limited acceleration control, i.e., $\|\mathbf{v}\| < \bar{v} = \sqrt{\frac{\bar{u}}{C_D}}$, and does not require to consider an explicit constraint on the velocity of the agents while designing bounded controllers as has been done in the literature.

We consider N_o static, convex polygonal obstacles \mathcal{O}_k , $k \in I_o = \{1, 2, \dots, N_o\}$, (grey colored polygons in Fig. 2), described as the convex hull of their vertices,

$$\mathcal{O}_k = \text{Conv} \left(\{\mathbf{r}_{ok}^1, \mathbf{r}_{ok}^2, \dots, \mathbf{r}_{ok}^{M_k}\} \right), \quad (3)$$

where $\text{Conv}(Q)$ is the convex hull of the points given in the set Q , $\mathbf{r}_{ok}^\ell = [x_{ok}^\ell \ y_{ok}^\ell]^T$ are the positions of the vertices for all $\ell \in \{1, 2, \dots, M_k\}$, M_k is the total number of vertices of \mathcal{O}_k , $k \in I_o$. The boundary of \mathcal{O}_k is denoted by $\partial\mathcal{O}_k$. Inspired from [6] and [7], the boundaries $\partial\mathcal{O}_k$ are inflated by a size of $\rho_{\bar{o}}$ ($> \rho_d$) to account for safety and agent size. The inflated obstacles are denoted by $\bar{\mathcal{O}}_k$, and are given as (Fig. 2): $\bar{\mathcal{O}}_k = \mathcal{O}_k \oplus B(\rho_{\bar{o}})$, where \oplus denotes the Minkowski sum of the sets and $B(\rho_{\bar{o}})$ denotes a ball of radius $\rho_{\bar{o}}$ centered at the origin. The boundary $\partial\bar{\mathcal{O}}_k$ of the inflated obstacle $\bar{\mathcal{O}}_k$ is a \mathcal{C}^1 curve for all $\rho_{\bar{o}} > 0$.

We consider the following problem of finding a near time-optimal trajectory for the agent operating under the dynamics in (1) and (2).

Problem 1 (Near Time-optimal trajectory). *Design a control action \mathbf{u} in analytical form such that the agent operating under dynamics (1) and (2) travels from an initial position \mathbf{r}_0 to final position \mathbf{r}_f in minimum time possible.*

In the next section, we give overview of the near time-optimal trajectory generation algorithm.

III. NEAR TIME-OPTIMAL TRAJECTORY

The near time-optimal trajectory between two given points is obtained by path-velocity decomposition [1], which consists of finding i) the shortest path, and ii) a near time-optimal velocity profile along the shortest path.

i) *Shortest paths*: We propose an approach wherein the kinematic and safety constraints are directly incorporated while constructing a special representation of the obstacle environment called \mathcal{C}^1 -Tangent graph, inspired from the idea of tangent graph [2]. The \mathcal{C}^1 -Tangent Graph (\mathcal{G}_{ct}) consists of \mathcal{C}^1 paths between any two nodes. For an obstacle environment with convex polygonal obstacles \mathcal{O}_k , the construction of the \mathcal{C}^1 -Tangent graph involves connecting the enlarged obstacles $\bar{\mathcal{O}}_k$ with their common tangents; then, the points at which these tangents touch the boundaries $\partial\bar{\mathcal{O}}_k$ serve as the nodes on \mathcal{G}_{ct} . Using \mathcal{G}_{ct} , one can find a path between any two nodes on \mathcal{G}_{ct} in the obstacle-free environment $\mathcal{W}_{free} = \mathcal{W} \setminus (\cup_{k=1}^{N_o} \mathcal{O}_k)$ using Dijkstra's algorithm [8]. The details of \mathcal{C}^1 -Tangent graph and shortest path are provided in section IV

ii) *Near time-optimal velocity profiles*: The shortest path between two points obtained using \mathcal{C}^1 -Tangent graph consists of straight line segments and circular arcs. Our goal is to obtain analytical expression for a near time-optimal velocity profile for each defender on its desired shortest path under bounded acceleration, to avoid huge computational cost that numerical integration schemes incur. We build on the approach described in [5], [9], adopting however the following different assumptions: 1) we consider a quadratic drag term in the dynamics, which apart from being a realistic assumption for aerial vehicles also imposes an inherent bound on the velocity; 2) we consider a constant bound on the norm of the acceleration instead of bounds on each component, as this is a more realistic assumption for under-actuated, multi-rotor vehicles such as quadrotors or hexacopters. We provide analytical expressions for the velocity bounds along a path, and for the time to traverse the path. The technical details on finding the near time-optimal velocity profiles on the shortest paths are given in Section V.

IV. \mathcal{C}^1 -TANGENT GRAPH AND SHORTEST PATH

The \mathcal{C}^1 -Tangent Graph \mathcal{G}_{ct} requires finding common tangents of the pairwise boundary curves $\partial\bar{\mathcal{O}}_k$, for all $k \in I_o$. We know that any two closed convex curves $\mathcal{C}_1, \mathcal{C}_2$ in 2D with non-overlapping interiors will have a maximum of four common tangent lines (Corollary 3.2 in [10]). To find the common tangents of the approximated convex

obstacles $\bar{\mathcal{O}}_k$, we formulate a novel quadratic function whose zeros give the locations at which the common tangents are tangent to the boundary curves $\partial\bar{\mathcal{O}}_k$ and $\partial\bar{\mathcal{O}}_{k'}$. The function is developed for general convex curves as detailed in Lemma 1.

Lemma 1 (Common Tangents). *Consider any two closed convex curves $\mathcal{C}_1, \mathcal{C}_2$ parameterized by $\mathcal{Y}_1 : [0, \Gamma_1] \rightarrow \mathbb{R}^2$ and $\mathcal{Y}_2 : [0, \Gamma_2] \rightarrow \mathbb{R}^2$, where $\mathcal{Y}_i(\gamma_i) = [x_i(\gamma_i), y_i(\gamma_i)]^T$ for $i = \{1, 2\}$. Define $f(\gamma_1, \gamma_2) = (m(\gamma_1, \gamma_2) - m_1(\gamma_1))^2 + (m(\gamma_1, \gamma_2) - m_2(\gamma_2))^2$, where $m(\gamma_1, \gamma_2) = \frac{y_2(\gamma_2) - y_1(\gamma_1)}{x_2(\gamma_2) - x_1(\gamma_1)}$ is the slope of the line joining $\mathcal{Y}_1(\gamma_1)$ and $\mathcal{Y}_2(\gamma_2)$, and for $i = \{1, 2\}$, $m_i(\gamma_i) = \frac{y_i'(\gamma_i)}{x_i'(\gamma_i)}$ is the slope of the tangent to \mathcal{C}_i at $\mathcal{Y}_i(\gamma_i)$, where $'$ denotes the derivative with respect to γ_i (see Fig. 1). The function f is locally convex and $f \geq 0, \forall [\gamma_1, \gamma_2]^T \in [0, \Gamma_1] \times [0, \Gamma_2]$. The solutions $\gamma^* = [\gamma_1^*, \gamma_2^*]^T$ to $f(\gamma_1, \gamma_2) = 0$ give the points through which common tangents to \mathcal{C}_1 and \mathcal{C}_2 pass.*

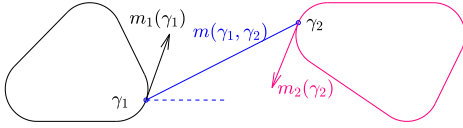


Figure 1: Common Tangent

Proof: We first prove the local convexity property of $f(\gamma_1, \gamma_2)$. The gradient of $f(\gamma_1, \gamma_2)$ is:

$$\nabla f(\gamma_1, \gamma_2) = \begin{bmatrix} 2((m - m_1)(m_{\gamma_1} - m_1') + (m - m_2)(m_{\gamma_1})) \\ 2((m - m_1)(m_{\gamma_2} + (m - m_2)(m_{\gamma_2} - m_2')) \end{bmatrix} \quad (4)$$

where $m_{\gamma_i} = \frac{\partial m}{\partial \gamma_i}$, for $i = \{1, 2\}$. We notice that the points (γ_1^*, γ_2^*) for which $f(\gamma_1^*, \gamma_2^*) = 0$ are also the points where the gradient of f vanishes because $m(\gamma_1^*, \gamma_2^*) = m_1(\gamma_1^*) = m_2(\gamma_2^*)$. The jacobian of f is:

$$\nabla^2 f(\gamma_1, \gamma_2) = \begin{bmatrix} f_{\gamma_1^2} & f_{\gamma_1 \gamma_2} \\ f_{\gamma_1 \gamma_2} & f_{\gamma_2^2} \end{bmatrix} \quad (5)$$

where

$$\begin{aligned} f_{\gamma_1^2} &= 2((m_{\gamma_1} - m_1')^2 + (m - m_1)(m_{\gamma_1^2} - m_1'') + (m_{\gamma_1})^2 \\ &\quad (m - m_2)m_{\gamma_1^2}) \\ f_{\gamma_2^2} &= 2((m_{\gamma_2} - m_2')^2 + (m - m_2)(m_{\gamma_2^2} - m_2'') + (m_{\gamma_2})^2 \\ &\quad (m - m_1)m_{\gamma_2^2}) \\ f_{\gamma_1 \gamma_2} &= 2((m_{\gamma_1} - m_1')m_{\gamma_2} + (m_{\gamma_2} - m_2')m_{\gamma_1} \\ &\quad (2m - m_1 - m_2)m_{\gamma_1 \gamma_2}) \end{aligned} \quad (6)$$

We have the determinant:

$$\det(\nabla^2 f(\gamma_1, \gamma_2))|_{(\gamma_1^*, \gamma_2^*)} = \left(4(m_{\gamma_1})^2(m_{\gamma_2})^2\right)|_{(\gamma_1^*, \gamma_2^*)} \geq 0. \quad (7)$$

This implies $f(\gamma_1, \gamma_2)$ is locally convex around the points (γ_1^*, γ_2^*) . It is very easy to see from the definition of $f(\gamma_1^*, \gamma_2^*)$ why the solutions to $f(\gamma_1, \gamma_2) = 0$ give coordinates of the points at which the two boundaries have a common tangent. ■

A nonlinear solver can provide the solutions to $f(\gamma_1, \gamma_2) = 0$ with appropriate initial conditions.

Let $P_r(\bar{\mathcal{O}}_k)$ denote the perimeter of the boundary $\partial\bar{\mathcal{O}}_k$. To find the common tangents, we parameterize the bound-

ary $\partial\bar{\mathcal{O}}_k$ by $\mathcal{Y}_k : [0, P_r(\bar{\mathcal{O}}_k)] \rightarrow \mathbb{R}^2$ given as:

$$\mathcal{Y}_k(\gamma) = \sum_{\ell=1}^{M_k} \tilde{\mathbb{B}}_k^\ell(\gamma) (\mathbf{r}_{\text{ok}}^\ell + \rho_{\bar{\mathcal{O}}} \hat{\mathbf{o}}(\psi_k^\ell(\gamma))) + \mathbb{B}_k^\ell(\gamma) (\mathbf{r}_{\text{ok}}^{2\ell} + \alpha_k^\ell(\gamma)(\mathbf{r}_{\text{ok}}^{2\ell+1} - \mathbf{r}_{\text{ok}}^{2\ell})) \quad (8)$$

where $\alpha_k^\ell(\gamma) = \frac{\gamma - \gamma_{\text{ok}}^{2\ell}}{\gamma_{\text{ok}}^{2\ell+1} - \gamma_{\text{ok}}^{2\ell}}$, $\tilde{\mathbb{B}}_k^\ell(\gamma)$ is 1 when $\gamma_{\text{ok}}^{2\ell-1} < \gamma < \gamma_{\text{ok}}^{2\ell}$ and 0 otherwise, $\mathbb{B}_k^\ell(\gamma)$ is 1 when $\gamma_{\text{ok}}^{2\ell} < \gamma < \gamma_{\text{ok}}^{2\ell+1}$ and 0 otherwise, and $\psi_k^\ell(\gamma) = \psi_{\text{ok}}^{2\ell-1} + \alpha_k^\ell(\gamma)(\psi_{\text{ok}}^{2\ell} - \psi_{\text{ok}}^{2\ell-1})$, where γ_{ok}^ℓ and ψ_{ok}^ℓ are the parameters as defined in Fig. 2 corresponding to the common points $\mathbf{r}_{\text{ok}}^\ell$ of circular and straight line segments on $\partial\bar{\mathcal{O}}_k$. Since all the common tangents would be the ones on the circular arcs of the approximated obstacles $\bar{\mathcal{O}}_k$ and $\bar{\mathcal{O}}_{k'}$, we initialize $\gamma_k, \gamma_{k'}$ to the values that correspond to the circular arcs of the boundaries $\partial\bar{\mathcal{O}}_k$ and $\partial\bar{\mathcal{O}}_{k'}$ in Lemma 1.

To reduce the search space for finding the shortest paths in the presence of circular obstacles, [4] proposes two filters: ellipse and convex-hull filter. We extend the ellipse filter to general convex polygonal obstacles. Let $L_s(\mathbf{r}_0, \mathbf{r}_f)$ be the length of the geodesic between the two points \mathbf{r}_0 and \mathbf{r}_f (solid red path in Fig. 2), and $L(\mathbf{r}_0, \mathbf{r}_f)$ be length of the straight line between \mathbf{r}_0 and \mathbf{r}_f (dotted pink line in Fig. 2). Denote the minimum distance between

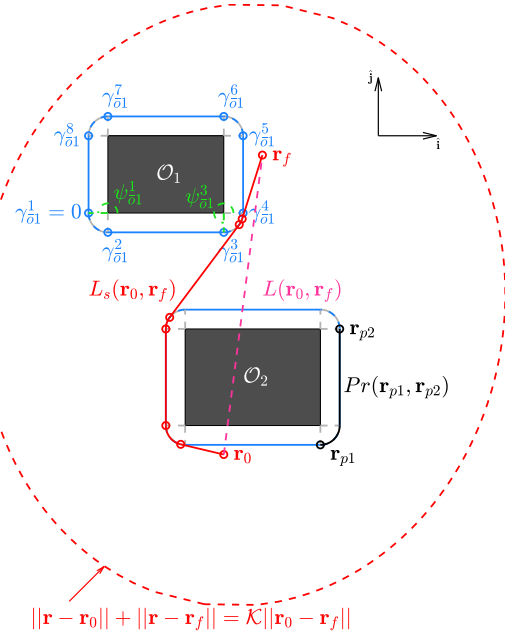


Figure 2: Shortest Path in an Obstacle Environment

the centroid of \mathcal{O}_k and any point on $\bar{\mathcal{O}}_k$ by ρ_k^{in} . Consider two points \mathbf{r}_{p_1} and \mathbf{r}_{p_2} on $\partial\bar{\mathcal{O}}_k$. Let $P_r(\mathbf{r}_{p_1}, \mathbf{r}_{p_2})$ be the perimeter of boundary curve between \mathbf{r}_{p_1} and \mathbf{r}_{p_2} , i.e., the smallest distance between the points \mathbf{r}_{p_1} and \mathbf{r}_{p_2} along the boundary $\partial\bar{\mathcal{O}}_k$ (Fig. 2).

■ **Lemma 2.** *One has: $L_s(\mathbf{r}_0, \mathbf{r}_f) \leq \mathcal{K}L(\mathbf{r}_0, \mathbf{r}_f)$, where*

$$\mathcal{K} = \max_{k \in \mathcal{I}_o} \left\{ \max_{\mathbf{r}_{p_1}, \mathbf{r}_{p_2} \in \partial\bar{\mathcal{O}}_k} \left\{ \frac{P_r(\mathbf{r}_{p_1}, \mathbf{r}_{p_2})}{R_{p_1}^{p_2}} \right\} \right\} \leq \max_{k \in \mathcal{I}_o} \left\{ \frac{P_r(\bar{\mathcal{O}}_k)}{4\rho_k^{in}} \right\}$$

with $P_r(\bar{\mathcal{O}}_k)$ being the perimeter of $\bar{\mathcal{O}}_k$.

Proof: The proof follows from the proof of Lemma 1 in [4]. The factor \mathcal{K} is the maximum ratio of the shortest perimeter with the distance of two points on the boundary of any obstacle. ■

The ellipse filter to find the shortest path can be applied by considering the obstacles lying completely inside the ellipse as given in Corollary 1 [4].

Corollary 1. *The shortest path between two points \mathbf{r}_p and \mathbf{r}_q lies inside the ellipse defined by $\|\mathbf{r}_p - \mathbf{r}\| + \|\mathbf{r}_q - \mathbf{r}\| = \mathcal{K}_m L_s(\mathbf{r}_p, \mathbf{r}_q)$, where $\mathcal{K}_m = \max_{k \in \mathcal{I}_o} \left\{ \frac{P_r(\mathcal{O}_k)}{4\rho_k^{in}} \right\}$.*

The \mathcal{C}^1 -Tangent graph \mathcal{G}_{ct} can be computed offline, and stored for finding the shortest paths using Dijkstra's algorithm [8]. Any shortest path \mathbf{P}_j , obtained using the \mathcal{C}^1 -Tangent graph, is associated with mappings $\mathcal{P}_j : [0, \Gamma^j] \rightarrow \mathbb{R}^2$ and $\vartheta_j : [0, \Gamma^j] \rightarrow [0, 2\pi]$, where Γ^j is the total length of the path \mathbf{P}_j . Here $\mathcal{P}_j(\gamma_j)$ gives the Cartesian coordinates, and $\vartheta_j(\gamma_j)$ gives the direction of the tangent to the path at the location reached after traveling γ_j distance along the path from the initial position.

When there are more than one agents moving on different shortest paths found using the \mathcal{C}^1 -Tangent graph, they might collide with each other. Whether they will collide with each other or not depends on whether the corresponding shortest paths intersect with each other. We have the following result regarding the intersection of the shortest paths.

Lemma 3. *Let \mathbf{P}_1 be the shortest path between the points \mathbf{r}_{11} and \mathbf{r}_{12} , and \mathbf{P}_2 be the shortest path between the points \mathbf{r}_{21} and \mathbf{r}_{22} . If \mathbf{P}_1 and \mathbf{P}_2 are obtained using the \mathcal{C}^1 -Tangent Graph then they intersect at most once.*

Proof: Case (1) - Both paths \mathbf{P}_1 and \mathbf{P}_2 are straight-line segments, i.e., there is no circular segment on either of these paths. This case is trivial as two lines intersect at most once, so any two line-segments of these paths would intersect each other at most once.

Case (2) - At least one of the two shortest paths has one or more circular segments. We prove this case by contradiction. Let us assume that there are 2 distinct collision segments on the two paths \mathbf{P}_1 and \mathbf{P}_2 . This is possible when these two paths converge towards each other, then diverge and then converge again. A possible scenario for this to happen is shown in Fig 3. Suppose \mathbf{P}_1 (solid blue, $\Gamma(\mathbf{P}_1) = 26.89m$) and \mathbf{P}_2 (solid red, $\Gamma(\mathbf{P}_2) = 25.00m$) are the two shortest paths joining \mathbf{r}_{11} to \mathbf{r}_{12} and \mathbf{r}_{21} to \mathbf{r}_{22} , respectively. These two paths as can be seen in Fig. 3 have two intersections. However, there exists a path $\hat{\mathbf{P}}_1$ (dotted blue) with total length $\Gamma(\hat{\mathbf{P}}_1) = 22.61m$ which would be the shortest path between \mathbf{r}_{11} to \mathbf{r}_{12} . This path has only one intersection with \mathbf{P}_2 . Similar argument can be applied to \mathbf{P}_2 and $\hat{\mathbf{P}}_2$ (dotted red, $\Gamma(\hat{\mathbf{P}}_2) = 24.97m$). The same observation can be made in case of multiple obstacles. This implies that the paths \mathbf{P}_1 and \mathbf{P}_2 intersect at most once. ■

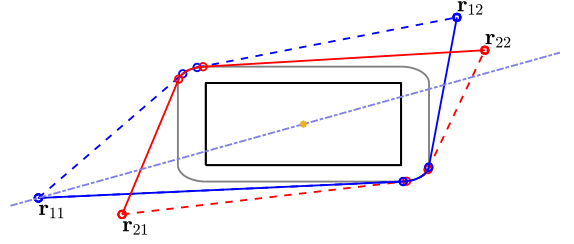


Figure 3: Shortest path intersection

V. NEAR TIME-OPTIMAL VELOCITY PROFILES UNDER BOUNDED ACCELERATION

Consider the shortest path \mathbf{P}_0^f from \mathbf{r}_0 to \mathbf{r}_f consisting of $N_{\mathbf{P}}^c$ circular arc segments, and $N_{\mathbf{P}}^s = N_{\mathbf{P}}^c + 1$ straight line segments. Let v_{2l-1} and v_{2l} be the speeds at the endpoints of the l^{th} circular segment, respectively, while moving forward along the path starting at the initial position. We formulate the problem of finding a near time-optimal velocity profile on the path from point \mathbf{r}_0 to point \mathbf{r}_f under bounded acceleration as a problem of finding the feasible terminal speed vector $\hat{\mathbf{v}} = [v_1, v_2, \dots, v_{2N_{\mathbf{P}}^c+1}, v_{2N_{\mathbf{P}}^c+2}]$ that minimizes the total time of travel. In the following, we discuss time-optimal control on straight line and near time-optimal control on circular segments with specified terminal speeds under acceleration constraint.

Minimum time on a straight line segment: For a straight line segment of length Γ_1 and the terminal speeds $v(0) = v_0$ and $v(\Gamma_1) = v_f$, the time-optimal control operates at either extremes [9], [11], i.e., $\|\mathbf{u}\| = \bar{u}$. The minimum time under this control action after integration is:

$$\tau_1(\Gamma_1, v_0, v_f) = \frac{1}{\sqrt{\bar{u}C_D}} \left(\tanh^{-1} \left(\frac{v_{sw}}{v_d} \right) + \tan^{-1} \left(\frac{v_{sw}}{v_d} \right) - \tanh^{-1} \left(\frac{v_0}{v_d} \right) - \tan^{-1} \left(\frac{v_f}{v_d} \right) \right), \quad (9)$$

where $v_{sw} = \sqrt{\frac{(\lambda-1)\bar{u}}{(\lambda+1)C_D}}$ is the speed at which the control action switches from one extreme to the other, and $\lambda = \left(\frac{\bar{u} + C_D v_f^2}{\bar{u} - C_D v_0^2} \right) e^{2C_D \Gamma_1}$.

Approximate minimum time on a circular segment: The dynamics of an agent along the path parametrized by $\mathbf{f}(\gamma)$ is:

$$\begin{aligned} \dot{\mathbf{r}} &= \mathbf{f}'(\gamma)v, \\ \dot{v} &= \mathbf{f}''(\gamma)\dot{\gamma} + \mathbf{f}'''(\gamma)v^2, \end{aligned} \quad (10)$$

where γ is the distance traveled along the path from the initial position, and v is the speed. Similar to [9], we consider double integrator dynamics along the path. But instead of constant bound on the acceleration along the path \dot{v} , we consider state dependent constraints on \dot{v} to ensure the acceleration \mathbf{u} satisfies the constraints (2), i.e.,

$$\begin{aligned} \dot{\gamma} &= v, \\ \dot{v} &= a, \end{aligned} \quad (11)$$

where $\|\mathbf{f}'(\gamma)a + \mathbf{f}''(\gamma)v^2 + C_D \mathbf{f}'''(\gamma)v^2\| < \bar{u}$. For a circu-

lar path of radius $\rho_{\bar{o}}$ centered at \mathbf{r}_c , we have:

$$\mathbf{f}'(\gamma) = \begin{bmatrix} -\sin(\alpha_0 + \frac{\gamma}{\rho_{\bar{o}}}) \\ \cos(\alpha_0 + \frac{\gamma}{\rho_{\bar{o}}}) \end{bmatrix}, \quad \mathbf{f}''(\gamma) = -\frac{1}{\rho_{\bar{o}}} \begin{bmatrix} \cos(\alpha_0 + \frac{\gamma}{\rho_{\bar{o}}}) \\ \sin(\alpha_0 + \frac{\gamma}{\rho_{\bar{o}}}) \end{bmatrix} \quad (12)$$

where α_0 is the orientation of the initial position vector with respect to \mathbf{r}_c . The constraint then reads:

$$-C_D v^2 - \sqrt{\bar{u}^2 - \frac{v^4}{\rho_{\bar{o}}^2}} \leq a \leq -C_D v^2 + \sqrt{\bar{u}^2 - \frac{v^4}{\rho_{\bar{o}}^2}}. \quad (13)$$

Suppose a defender has to travel a circular segment of length Γ_2 and the terminal speeds on this path are $v(0) = v_0$ and $v(\Gamma_2) = v_f$. The time-optimal control for the trajectories of (11) is a bang-bang control with acceleration a operating at its extreme values based on a switching condition [11]. However, this requires integration of the system (11) under the extreme accelerations given in (13) to find the switching condition and required total minimum time. This involves inverting hypergeometric functions, which would be computationally intensive, so we approximate the acceleration bounds as:

$$-C_D v^2 - \left(\frac{\bar{u}^2 \rho_{\bar{o}}^2 - v^4}{\bar{u} \rho_{\bar{o}}^2} \right) \leq a \leq -C_D v^2 + \left(\frac{\bar{u}^2 \rho_{\bar{o}}^2 - v^4}{\bar{u} \rho_{\bar{o}}^2} \right). \quad (14)$$

It is easy to verify that the acceleration a satisfying the constraints in (14) also satisfies the constraints in (13).

The minimum time required to travel a circular segment of length Γ_2 with terminal speeds v_0 and v_f after integrating (11) with approximate extreme accelerations in (14) is:

$$\tau_2(\Gamma_2, v_0, v_f) = \frac{1}{\lambda_3} \left(\frac{\tan^{-1}(\lambda_1^\circ v_{sw})}{\lambda_1} + \frac{\tanh^{-1}(\lambda_2^\circ v_{sw})}{\lambda_2} \right) - \frac{1}{\lambda_3} \left(\frac{\tan^{-1}(\lambda_1^\circ v_0)}{\lambda_1} + \frac{\tanh^{-1}(\lambda_2^\circ v_0)}{\lambda_2} \right) + \frac{1}{\lambda_3} \left(\frac{\tan^{-1}(\lambda_2^\circ v_f)}{\lambda_2} + \frac{\tanh^{-1}(\lambda_1^\circ v_f)}{\lambda_1} \right) - \frac{1}{\lambda_3} \left(\frac{\tan^{-1}(\lambda_2^\circ v_{sw})}{\lambda_2} + \frac{\tanh^{-1}(\lambda_1^\circ v_{sw})}{\lambda_1} \right), \quad (15)$$

where $v_{sw} = \sqrt{\frac{\kappa_1(e_\kappa+1) + \sqrt{(\kappa_1(e_\kappa+1))^2 - (e_\kappa-1)^2(\kappa_1^2 - \kappa_2^2)}}{2(e_\kappa-1)}}$ is the speed at which the control action switches from one extreme to the other, $e_\kappa = e^{\frac{\kappa}{\kappa_0}}$, $\kappa = \Gamma_2 + 2\kappa_0 \tanh^{-1}\left(\frac{\kappa_2 - 2v_0^2}{\kappa_1}\right) - 2\kappa_0 \tanh^{-1}\left(\frac{\kappa_2 - 2v_f^2}{\kappa_1}\right)$, $\kappa_0 = \frac{\rho_{\bar{o}}}{2\lambda_0}$, $\kappa_1 = \rho_{\bar{o}}\bar{u}\lambda_0$, $\kappa_2 = C_D\rho_{\bar{o}}^2\bar{u}$, $\lambda_1 = \sqrt{\rho_{\bar{o}}(\lambda_0 - \rho_{\bar{o}}C_D)}$, $\lambda_2 = \sqrt{\rho_{\bar{o}}(\lambda_0 + \rho_{\bar{o}}C_D)}$, $\lambda_3 = \frac{\lambda_0}{\rho_{\bar{o}}}\sqrt{\frac{\bar{u}}{2}}$, $\lambda_1^\circ = \frac{\sqrt{2}}{\lambda_1\sqrt{\bar{u}}}$, $\lambda_2^\circ = \frac{\sqrt{2}}{\lambda_2\sqrt{\bar{u}}}$, and $\lambda_0 = \sqrt{\rho_{\bar{o}}^2 C_D^2 + 4}$.

For each segment on the path, one can find the \mathcal{C}^0 velocity profile that satisfies acceleration bound and approximately minimizes the total travel time for the given terminal speeds. Let the total time required to travel \mathbf{P}_0^f under $\tilde{\mathbf{v}}$ be:

$$\tau(\mathbf{P}_0^f, \tilde{\mathbf{v}}) = \sum_{l=1}^{N_{\mathbf{P}}} \tau_{i_l}(\Gamma_l, v_l, v_{l+1}) \quad (16)$$

where $i_l = \frac{3+(-1)^l}{2}$, $N_{\mathbf{P}} = 2N_{\mathbf{P}}^c + 2$. The terminal speed

vector $\tilde{\mathbf{v}}$ is found by solving:

$$\begin{aligned} & \text{Minimize} \quad \tau(\mathbf{P}_0^f, \tilde{\mathbf{v}}) \\ & \text{Subject to} \quad 1) \Gamma_l \geq \begin{cases} \log\left(\frac{\bar{u} - C_D v_l^2}{\bar{u} - C_D v_{l+1}^2}\right), & \text{if } v_l < v_{l+1} \\ \log\left(\frac{\bar{u} + C_D v_l^2}{\bar{u} + C_D v_{l+1}^2}\right), & \text{if } v_l \geq v_{l+1} \end{cases} \\ & \quad \forall l \in \{1, 3, \dots, N_{\mathbf{P}}\} \\ & \quad 2) \Gamma_l \geq \begin{cases} \Gamma^+(v_l, v_{l+1}), & \text{if } v_l < v_{l+1} \\ \Gamma^-(v_l, v_{l+1}), & \text{if } v_l \geq v_{l+1} \end{cases} \\ & \quad \forall l \in \{2, 4, \dots, N_{\mathbf{P}}\} \\ & \quad 3) v_l \in [0, \bar{v}^c], \forall l \in \{2, 3, \dots, N_{\mathbf{P}} - 1\} \end{aligned} \quad (17)$$

where $\Gamma^+(v_1, v_2) = \frac{\rho_{\bar{o}}(\tanh^{-1}(\eta^+(v_2)) - \tanh^{-1}(\eta^+(v_1)))}{\lambda_0}$, $\Gamma^-(v_1, v_2) = \frac{\rho_{\bar{o}}(\tanh^{-1}(\eta^-(v_2)) - \tanh^{-1}(\eta^-(v_1)))}{\lambda_0}$, $\eta^+(v) = \frac{C_D\rho_{\bar{o}}^2\bar{u} + 2(v)^2}{\lambda_0(\bar{v}^c)^2}$ and $\eta^-(v) = \frac{C_D\rho_{\bar{o}}^2\bar{u} - 2(v)^2}{\lambda_0(\bar{v}^c)^2}$, and maximum possible speed on the circular segment $\bar{v}^c = \sqrt{\frac{\sqrt{C_D^2\rho_{\bar{o}}^4 + 4\bar{u}^2\rho_{\bar{o}}^2} - C_D\rho_{\bar{o}}^2}{2}}$. The near time-optimal velocity profile is determined as:

$$\tilde{\mathbf{v}}_0^f = \arg \min_{\tilde{\mathbf{v}}} \left(\tau(\mathbf{P}_0^f, \tilde{\mathbf{v}}) \right). \quad (18)$$

The solution to (17) will have maximum possible speeds in the feasible set along the given path to ensure that the total travel time is minimized. For simplicity, we chose $v_1 = v_{2N_{\mathbf{P}}^c+2} = 0$, however this approach can be applied to any feasible non-zero initial and final speeds. The terminal speed vector that maximizes the speeds along the path with the given acceleration constraints can be obtained using Algorithm 1.

VI. CONCLUSION

We developed \mathcal{C}^1 -Tangent graph for an obstacle environment which provides continuously differentiable (\mathcal{C}^1) path between any two nodes. We developed a novel quadratic function to find common tangents of the obstacle boundaries in \mathcal{C}^1 -Tangent graph. We also extended the ellipse filter to more generic environments with convex obstacles to reduce search time of an algorithm finding shortest path on \mathcal{C}^1 -Tangent graph.

We provide analytical expressions for the near time-optimal velocity profiles for the agents moving on a shortest path obtained on \mathcal{C}^1 -Tangent graph under damped double integrator dynamics with bounded acceleration.

REFERENCES

- [1] K. Kant and S. W. Zucker, "Toward efficient trajectory planning: The path-velocity decomposition," *The international journal of robotics research*, vol. 5, no. 3, pp. 72–89, 1986.
- [2] Y.-H. Liu and S. Arimoto, "Path planning using a tangent graph for mobile robots among polygonal and curved obstacles: Communication," *The International Journal of Robotics Research*, vol. 11, no. 4, pp. 376–382, 1992.
- [3] T. Kröger, "Literature survey: Trajectory generation in and control of robotic systems," in *On-Line Trajectory Generation in Robotic Systems*. Springer, 2010, pp. 11–31.
- [4] D.-S. Kim, K. Yu, Y. Cho, D. Kim, and C. Yap, "Shortest paths for disc obstacles," in *International Conference on Computational Science and Its Applications*. Springer, 2004, pp. 62–70.
- [5] T. Kunz and M. Stilman, "Time-optimal trajectory generation for path following with bounded acceleration and velocity," *Robotics: Science and Systems VIII*, pp. 1–8, 2012.

Algorithm 1: Near time-optimal velocity on path \mathbf{P}

Input: \mathbf{P} , $N_{\mathbf{P}}^c$, \bar{u} , C_D **Output:** $\bar{\mathbf{v}} = [0, v_2, v_3, \dots, v_{2N_{\mathbf{P}}^c+1}, 0]$ 1 $i = 1$, $j = 2N_{\mathbf{P}}^c + 2$; $v_i = v_j = 0$;2 **while** $v_i < \bar{v}^c$ & $i \leq 2N_{\mathbf{P}}^c + 2$ **do**3 $v_{i+1} =$
4 $\sqrt{\frac{1}{2} \left(\kappa_1 \tanh\left(\frac{\Gamma_i \lambda_0}{\rho_{\bar{v}}} + \tanh^{-1}\left(\frac{\kappa_2 + 2v_i^2}{\kappa_1}\right)\right) - \kappa_2 \right)}$
5 **if** i *is odd* (i.e., *straight segment*) **then**
6 $v_{i+1} = \sqrt{\frac{(\bar{u} - e^{-2C_D \Gamma_i} (\bar{u} - C_D v_i^2))}{C_D}}$
7 **if** *acceleration beyond* \bar{v}^c *possible* **then**
8 $v_{i+1} = \bar{v}^c$ 8 $i = i + 1$;9 **while** $v_j < \bar{v}^c$ **do**10 $v_{j-1} =$
11 $\sqrt{\frac{1}{2} \left(\kappa_2 - \kappa_1 \tanh\left(-\frac{\Gamma_i \lambda_0}{\rho_{\bar{v}}} + \tanh^{-1}\left(\frac{\kappa_2 - 2v_i^2}{\kappa_1}\right)\right) \right)}$
12 **if** $j - 1$ *is odd* **then**
13 $v_{j-1} = \sqrt{\frac{(-\bar{u} + e^{-2C_D \Gamma_i} (\bar{u} + C_D v_i^2))}{C_D}}$
14 **if** *deceleration to 0 from* \bar{v}^c *possible* **then**
15 $v_{j-1} = \bar{v}^c$ 15 $j = j - 1$;16 $v_k = \bar{v}^c$ for all k such that $i < k < j$ 17 **return** $\bar{\mathbf{v}} = [v_1, v_2, v_3, \dots, v_{2N_{\mathbf{P}}^c+1}, v_{2N_{\mathbf{P}}^c+2}]'$

- [6] R. Hegde and D. Panagou, "Multi-agent motion planning and coordination in polygonal environments using vector fields and model predictive control," in *2016 European Control Conference (ECC)*. IEEE, 2016, pp. 1856–1861.
- [7] W. D. Esquível and L. E. Chiang, "Nonholonomic path planning among obstacles subject to curvature restrictions," *Robotica*, vol. 20, no. 1, pp. 49–58, 2002.
- [8] T. H. Cormen, C. E. Leiserson, R. L. Rivest, and C. Stein, *Introduction to algorithms*. MIT press, 2009.
- [9] J. Peng and S. Akella, "Coordinating multiple double integrator robots on a roadmap: Convexity and global optimality," in *Proceedings 2005 IEEE International Conference on Robotics and Automation*. IEEE, 2005, pp. 2751–2758.
- [10] G. Czédli and L. L. Stachó, "A note and a short survey on supporting lines of compact convex sets in the plane," *arXiv preprint arXiv:1612.01453*, 2016.
- [11] A. E. Bryson and H. Y. Chi, *Applied optimal control: optimization, estimation and control*. Hemisphere, Washington D.C., 1975.